J Appl Physiol 113: 114–123, 2012.
First published April 19, 2012; doi:10.1152/japplphysiol.00431.2011.

Deficiency of inducible nitric oxide synthase attenuates immobilization-induced skeletal muscle atrophy in mice

Sang-Keun Bae,[1] Hey-Na Cha,[2,3] Tae-Jin Ju,[2,3] Yong-Woon Kim,[2] Hee Sun Kim,[4] Yong-Dae Kim,[5] Jin-Myoung Dan,[6] Jong-Yeon Kim,[2] Se-dong Kim,[1] and So-Young Park[2,3]

[1]*Department of Orthopedic Surgery,* [2]*Department of Physiology,* [3]*Aging-Associated Vascular Disease Research Center,* [4]*Department of Microbiology, and* [5]*Department of Otorhinolaryngology, College of Medicine, Yeungnam University, Daegu, Korea; and* [6]*Department of Orthopedic Surgery, Gumi CHA University Hospital, Gumi, Korea*

Submitted 8 April 2011; accepted in final form 13 April 2012

Bae S-K, Cha H-N, Ju T-J, Kim Y-W, Kim HS, Kim Y-D, Dan J-M, Kim J-Y, Kim S-d, Park S-Y. Deficiency of inducible nitric oxide synthase attenuates immobilization-induced skeletal muscle atrophy in mice. *J Appl Physiol* 113: 114–123, 2012. First published April 19, 2012; doi:10.1152/japplphysiol.00431.2011.—The present study examined the effects of inducible nitric oxide synthase (iNOS) deficiency on skeletal muscle atrophy in single leg-immobilized iNOS knockout (KO) and wild-type (WT) mice. The left leg was immobilized for 1 wk, and the right leg was used as the control. Muscle weight and contraction-stimulated glucose uptake were reduced by immobilization in WT mice, which was accompanied with increased iNOS expression in skeletal muscle. Deficiency of iNOS attenuated muscle weight loss and the reduction in contraction-stimulated glucose uptake by immobilization. Phosphorylation of Akt, mTOR, and p70S6K was reduced to a similar extent by immobilization in both WT and iNOS KO mice. Immobilization decreased FoxO1 phosphorylation and increased mRNA and protein levels of MuRF1 and atrogin-1 in WT mice, which were attenuated in iNOS KO mice. Aconitase and superoxide dismutase activities were reduced by immobilization in WT mice, and deficiency of iNOS normalized these enzyme activities. Increased nitrotyrosine and carbonylated protein levels by immobilization in WT mice were reversed in iNOS KO mice. Phosphorylation of ERK and p38 was increased by immobilization in WT mice, which was reduced in iNOS KO mice. Immobilization-induced muscle atrophy was also attenuated by an iNOS-specific inhibitor N^6-(1-iminoethyl)-L-lysine, and this finding was accompanied by increased FoxO1 phosphorylation and reduced MuRF1 and atrogin-1 levels. These results suggest that deficiency of iNOS attenuates immobilization-induced skeletal muscle atrophy through reduced oxidative stress, and iNOS-induced oxidative stress may be required for immobilization-induced skeletal muscle atrophy.

muscle atrophy; MuRF; atrogin; oxidative stress

SKELETAL MUSCLE is the largest organ in the human body, accounting for 40% of body mass and exhibits a very high level of plasticity. Resistance exercise leads to skeletal muscle hypertrophy characterized by increased muscle size, protein contents, and strength (23, 25, 31). On the contrary, prolonged period of skeletal muscle inactivity due to immobilization, hindlimb unloading, or nerve injury can result in loss of muscle mass, commonly known as muscle atrophy (7, 33). Characteristic features of skeletal muscle atrophy include a decrease in fiber cross-sectional area, myofibrillar protein contents, and strength, and it leads to increased fragility and insulin resistance (23, 25, 31). Although skeletal muscle atrophy is caused by a variety of factors, reduced protein synthesis, increased protein degradation, or a combination of reduced protein synthesis and increased protein degradation involve a common pathological process to cause atrophy (62). Two weeks of unilateral limb immobilization in healthy men and women downregulates the gene involved in protein synthesis and upregulates genes involved in protein degradation (1).

Many studies rely on rodent animal models, and some of them are suitable models for studying disease-related atrophy such as cachexia with cancer, diabetes, and denervation. However, in these cases, the concurrent presence of systemic alteration may make it difficult to study the mechanism of atrophy. Although bilateral hindlimb immobilization is complex and invasive, and may cause stress-induced systemic alteration, single-leg immobilization is a simple and reliable method (13, 33).

Nitric oxide (NO) is a gas molecule that plays critical roles as a mediator of physiological processes including neural signaling, immune modulation, and vasoregulation (36). NO is synthesized enzymatically by three isoforms of nitric oxide synthase (NOS): endothelial NOS (eNOS), neuronal NOS (nNOS), and inducible NOS (iNOS) (54). While eNOS and nNOS are constitutively present, iNOS produces greater amounts of NO compared with eNOS and nNOS and is highly induced under various pathological conditions (27). All three isoforms of NOS are expressed in skeletal muscles (42, 48), and a low level of NO is integrated into physiological functions such as contraction and metabolism (35, 42). Although the expression level of iNOS is very low in skeletal muscle of normal rodent and human (14), overproduction of NO by elevated iNOS expression may be involved in muscle atrophy. The expression of iNOS is elevated in the quadriceps muscles of chronic obstructive pulmonary disease patients with low body weight compared with patients with normal body weight (3). Skeletal muscle wasting of type 2 diabetes and congestive heart failure is also accompanied with increased iNOS expression in skeletal muscle (2, 53). Moreover, the alcohol-induced skeletal muscle atrophy in rats is accompanied by increased iNOS expression in atrophic muscle (57). On this background, we hypothesized that iNOS may be involved in immobilization-induced skeletal muscle atrophy, and the suppression of iNOS prevents atrophy. In the present study, the effects of deficiency of iNOS on immobilization-induced skeletal muscle atrophy was examined in single leg-immobilized iNOS knockout and wild-type mice.

Address for reprint requests and other correspondence: S.-Y. Park, Dept. of Physiology, Yeungnam Univ. College of Medicine, Daegu 705-717, South Korea (e-mail: sypark@med.yu.ac.kr).

MATERIALS AND METHODS

Animals. Male wild-type and iNOS knockout (The Jackson Laboratory, Bar Harbor, ME) 4-mo-old mice were housed in a room with a 12:12-h light/dark cycle, lights on at 0700 and off at 1900. All the mice were fed a standard chow diet with free access to water. Mice were anesthetized by an intraperitoneal injection of tiletamine and zolezepam (25 mg/kg) and xylazine (10 mg/kg) before the immobilization procedure. The left hindlimb of each mouse was wrapped with self-adhering elastic wrap (3M, St. Paul, MN), encased in a plastic stick made from a microcentrifuge tube, and then the plastic stick was fixed with surgical tape. The right hindlimb of each mouse served as its own control. Immobilization was maintained for 6 h or 1 wk. At the end of the immobilization, mice were anesthetized, and blood was collected from retroorbital plexus using microhematocrit capillary tubes coated with heparin. Blood was centrifuged and plasma was stored at −80°C for further analysis. Then skeletal muscles were excised, weighted, and used in experiments immediately or stored at −80°C for further analysis. The effect of the iNOS selective inhibitor N^6-(1-iminoethyl)-L-lysine (L-NIL; Cayman Chemical, Ann Arbor, MI, USA) on skeletal muscle atrophy was tested after intraperitoneal injection of L-NIL (10 $mg \cdot kg^{-1} \cdot day^{-1}$) into mice once a day during the immobilization period (10, 58). L-NIL was injected before the immobilization procedure, and saline was injected in control mice. This study was conducted in accordance with the guidelines for the care and use of laboratory animals provided by Yeungnam University, and all experimental protocols were approved by the Ethics Committee of Yeungnam University.

In situ muscle contraction-stimulated glucose uptake. Four days before contraction experiment, single leg-immobilized mice were anesthetized by intraperitoneal injection of anesthetics (tiletamine and zolezepam, 25 mg/kg body wt; xylazine, 10 mg/kg body wt), and a silicone catheter (Helix Medical, Carpinteria, CA) was inserted into right jugular vein. On the day of the experiment, a Y-connector was connected to the jugular vein catheter to deliver ^{14}C-labeled 2-deoxy-D-glucose (2-[1-^{14}C]DG; PerkinElmer Life and Analytical Sciences, Boston, MA) to measure in vivo skeletal muscle glucose uptake (28). An electrical stimulation experiment was conducted to induce muscle contraction 7 days after immobilization. After anesthetizing mice, gastrocnemius muscles of both hindlimbs were exposed, electrodes were inserted into muscles, and 10 μCi of 2-[1-^{14}C]DG was injected into the catheter right before electrical stimulation. A 5-V stimulation was delivered with a 0.1-s duration and a frequency of 100 Hz. The muscle was stimulated for 10 s and rested for 10 s, which was repeated for 10 min (28, 56). Both muscles were removed 35 min after 2-[1-^{14}C]DG injection and used for analysis of contraction-stimulated glucose uptake. Plasma glucose concentration was measured from tail blood using a Beckman Glucose Analyzer 2 (Beckman, Fullerton, CA) before and after electrical stimulation. Because 2-DG is a glucose analog that is phosphorylated but not metabolized, electrically stimulated glucose uptake in skeletal muscle can be estimated by determining the tissue content of 2-[^{14}C]DG-6-*P*. On this basis, glucose uptake in individual tissues was calculated from the plasma 2-[^{14}C]DG profile, which was fitted with a double-exponential or linear curve by using MLAB (Civilized Software, Bethesda, MD) and tissue 2-[^{14}C]DG-6-*P* content. Plasma concentrations of 2-[^{14}C]DG was determined after deproteinization of plasma samples at 5, 10, 15, 25, and 35 min after 2-[^{14}C]DG injection (49).

Quantitative real time polymerase chain reaction (qRT-PCR). Skeletal muscle (~25 mg) was homogenized in TRI reagent (Sigma-Aldrich, St. Louis, MO) using an Ultra-Turrax T25 (Janke and Kunkel, IKA-Labortechnik, Staufel, Germany). RNA was reverse transcribed to cDNA from 1 μg of total RNA by using a High-Capacity cDNA Reverse Transcription Kit (Applied Biosystems, Foster City, CA). Quantitative real-time PCR was performed using the Real-Time PCR 7500 System and Power SYBR Green PCR Master Mix (Applied Biosystems) according to the manufacturer's instructions. The cycle at which the abundance of the accumulated PCR product crossed a specific threshold, the threshold cycle (C_T), was determined, and the difference in C_T values between β-actin and target gene was calculated for each sample. β-Actin was used as a housekeeping gene in this experiment and was not different between control and immobilization. Each reaction mixture was incubated at 95°C for 10 min followed by 45 cycles of 95°C for 15 s, 55°C for 20 s, and 72°C for 35 s. Sequences of primers for β-actin, iNOS, atrogin-1, and muscle ring finger-1 (MuRF1) were based on the National Center for Biotechnology Information nucleotide database (NCBI) and were designed using the Primer Express Program (Applied Biosystems): β-actin (121 bp: forward, 5′-TGG ACA GTG AGG CAA GGA TAG-3′; reverse, 5′-TAC TGC CCT GGC TCC TAG CA-3′), iNOS (71 bp: forward, 5′-CTC CTG CCT CAT GCC ATT-3′; reverse, 5′-TGT TCC TCT ATT TTT GCC TCT TTA-3′), atrogin-1 (71 bp: forward, 5′-GTT CAC AAA GGA AGT ACG AAG G-3′; reverse, 5′-GAA GTC CAG TCT GTT GAA AGC TT-3′), and MuRF1 (71 bp: forward, 5′-CGT GCA GAG TGA CCA AGG-3′; reverse, 5′-GCG TAG AGG GTG TCA AAC TTC-3′). The reactions for eNOS and nNOS used the same conditions as with iNOS, except for the annealing temperature, which was 52°C instead of 55°C. Primers for β-actin, eNOS, and nNOS were also based on NCBI's nucleotide database and were designed using the Primer Express Program (Applied Biosystems): mouse β-actin (71 bp: forward, 5′-CCA ACC GTG AAA AGA TGA-3′; reverse, 5′-CTG GAT GGC TAC GTA CAT G-3′), eNOS (71 bp: forward, 5′-CCA ACC GTG AAA AGA TGA-3′; reverse, 5′-CTG GAT GGC TAC GTA CAT G-3′), nNOS (71 bp: forward, 5′-GGC TGT GCT TTG ATG GA-3′; reverse, 5′-TGA ATC GGA CCT TGT AGC T-3′).

Western blotting. Antibodies for Akt, phosphorylated Akt (p-Akt), mammalian target of rapamycin (mTOR), p-mTOR, 70-kDa ribosomal protein S6 kinase (p70S6K), p-p70S6K, forkhead box O1 (FoxO1), p-FoxO1, MuRF1, atrogin-1, extracellular signal-related kinase (ERK), p-ERK, p38, and p-p38 were purchased from Cells Signaling Technologies (Danvers, MA). Antibodies for iNOS and gyceraldehyde 3-phosphate dehydrogenase (GAPDH) were purchased from Santa Cruz Biotechnology (Santa Cruz, CA), and nitrotyrosine antibody was purchased from Upstate Biotechnology (Lake Placid, NY). Muscles (~25 mg) were homogenized in lysis buffer (Invitrogen, Carlsbad, CA) containing 1% NP40, 150 mM NaCl, 5 mM MgCl, 10 mM HEPES, leupeptin, and pepstatin A. Protein sample was separated by 10% sodium dodecyl sulfate-polyacrylamide gel electrophoresis (SDS-PAGE). Resolved proteins were then transferred to a 0.45-μm polyvinylidene fluoride membrane (PVDF; Millipore, Billerica, MA). After blocking with a solution containing 5% skim milk in TBST [10 mM Tris·HCl (pH 7.4), 150 mM NaCl, and 0.1% Tween-20], the membrane was incubated overnight at 4°C with the primary antibodies except for the GAPDH antibody, in which the membrane was incubated for 1 h at room temperature. The specific antibody binding was detected using sheep anti-rabbit IgG horseradish peroxidase or goat anti-mouse IgG houseradish peroxidase (Bio-Rad, Hercules, CA) for 1 h at room temperature except for nitrotyrosine, for which mouse anti-mouse IgG horseradish peroxidase (Bio-Rad) was used. After addition of chemiluminescence detection regent (Millipore), signals were recorded and quantified using LAS-3000 image analyzer and Multi Guage 3.0 software (Fujifilm, Tokyo, Japan).

Protein carbonylation. Protein carbonylation was measured with an OxyBlot Protein Oxidation Detection kit (Chemicon, Temecula, CA) according to the manufacturer's instructions. Briefly tissues were homogenized in lysis buffer (Invitrogen) with 50 mM dithiothreitol. Ten micrograms of protein in 3 μl lysis buffer was added to 3 μl of 12% SDS. Samples were derivatized by adding 6 μl of 2,4-dinitrophenylhydrazine solution and incubating at room temperature for 15 min, followed by addition of 4.5 μl of neutralization solution. The protein sample was separated by 12% SDS-PAGE and then transferred to a 0.45-μg PVDF membrane. The membrane was blocked

with 1% bovine serum albumin (BSA) in TBST. After blocking with a 1% BSA in TBST, the membrane was incubated for 1 h at room temperature with rabbit anti-2,4-dinitrophenyl antibody diluted 1:150 in 1% BSA/TBST, washed with TBST, then incubated for 1 h at room temperature with goat anti-rabbit IgG coupled to horseradish peroxidase. Carbonylated protein was visualized by the same method described in Western blotting.

Nitrite and nitrate. Plasma concentrations of the NO-derived end products nitrite and nitrate were measured by a Total NO Assay Kit (R&D Systems, Minneapolis, MN). To minimize interference with plasma protein, the sample was ultrafiltered through a 10,000-Da cut-off filter (Millipore) prior to the assay.

Superoxide dismutase (SOD) activity. Mice were perfused with 10 ml ice-cold phosphate buffered saline (PBS), and muscle samples were rapidly harvested and washed with PBS to remove red blood cells and clots. The muscle was minced in ice-cold buffer (20 mM HEPES, pH 7.2, 1 mM EGTA, 210 mM mannitol, and 70 mM sucrose), homogenized with glass-Teflon motorized homogenizer, and centrifuged at 1,500 *g* for 5 min at 4°C. The supernatant was collected and centrifuged at 10,000 *g* for 15 min at 4°C. The precipitated pellet containing mitochondria was resuspended and homogenized. MnSOD activity was measured with Superoxide Dismutase Assay Kit (Cayman, Ann Arbor, MI) according to the manufacturer's instructions. The kit utilizes a tetrazolium salt for detection of superoxide radicals generated by xanthine oxidase and hypoxanthine.

Aconitase activity. Aconitase activity was measured using Aconitase Assay Kit (Cayman) according to manufacturer's instructions. The kit utilizes the formation of NADPH using isocitrate as a substrate. Briefly, muscle sample was minced in ice-cold buffer, homogenized with glass-Teflon motorized homogenizer, and centrifuged at 800 *g* for 10 min at 4°C. The supernatant was collected and centrifuged at 20,000 *g* for 10 min at 4°C. The precipitated pellet containing mitochondria was resuspended, sonicated for 20 s, and used for aconitase activity assay.

Statistical analysis. Data are expressed as means ± SE. The difference among groups was analyzed using one-way ANOVA followed by Scheffé's post hoc test. Statistical significance was at $P < 0.05$.

RESULTS

Skeletal muscle mass and contraction-stimulated glucose uptake. Food intake and body weight were not significantly affected by the immobilization procedure, and they were not different between wild-type and iNOS knockout mice before and after immobilization. Body weight was 29.5 ± 0.56 and 28.3 ± 0.71 g in wild-type and iNOS knockout, respectively, on the last day of immobilization, and average daily food intake was 3.3 ± 0.12 and 3.2 ± 0.13 g in wild-type and iNOS knockout, respectively, during the immobilization period. The weights of gastrocnemius and quadriceps muscles that were corrected for whole body weight were reduced by 19% and 28%, respectively, in wild-type mice after 1 wk immobilization compared with that of the control leg. The skeletal muscle mass of iNOS knockout mice was also reduced by 9% and 16% in gastrocnemius and quadriceps muscles, respectively, by immobilization. However, the skeletal muscle mass of iNOS knockout mice was significantly higher than wild-type mice after immobilization (Fig. 1, *A* and *B*). Contraction-stimulated glucose uptake was measured to determine muscle function in both control and immobilized legs. Contraction-stimulated glucose uptake was not different between wild-type and iNOS knockout mice in control legs. While immobilization significantly reduced contraction-stimulated glucose uptake in wild-type mice, lack of iNOS attenuated the reduction of contraction-stimulated glucose uptake by immobilization (Fig. 1*C*).

NOS expression. Gene expression of iNOS was increased in immobilized leg compared with control leg in wild-type mice. While iNOS protein was not detected in iNOS knockout mice, the protein level of iNOS was increased in immobilized leg compared with control leg in wild-type mice. The gene expression of eNOS and nNOS was not different among the groups (Fig. 2).

Protein synthesis and degradation. Signaling pathways involved in protein synthesis and degradation were measured at 6 h and 1 wk after immobilization to determine whether

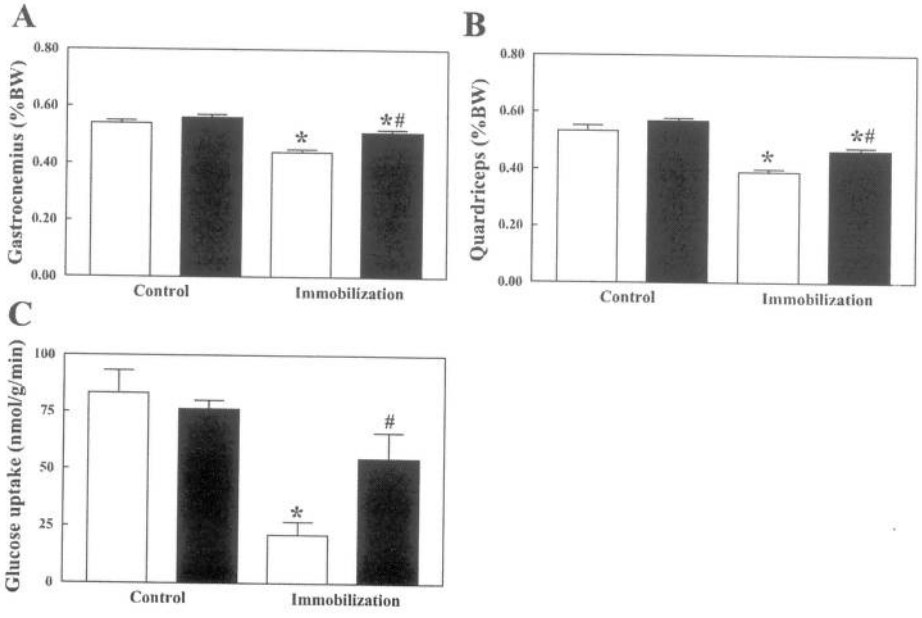

Fig. 1. Skeletal muscle mass and contraction-stimulated glucose uptake in wild-type (open bar) and inducible nitric oxide synthase knockout (iNOS KO; filled bar) mice after 1 wk immobilization. The weights of gastrocnemius (*A*) and quadriceps muscles (*B*) were corrected for body weight (BW). Muscle glucose uptake was measured under contraction induced by electrical stimulation (*C*). Data are means ± SE for 7–11 mice for each group. *$P < 0.05$ vs. wild-type control; #$P < 0.05$ vs. wild-type immobilization.

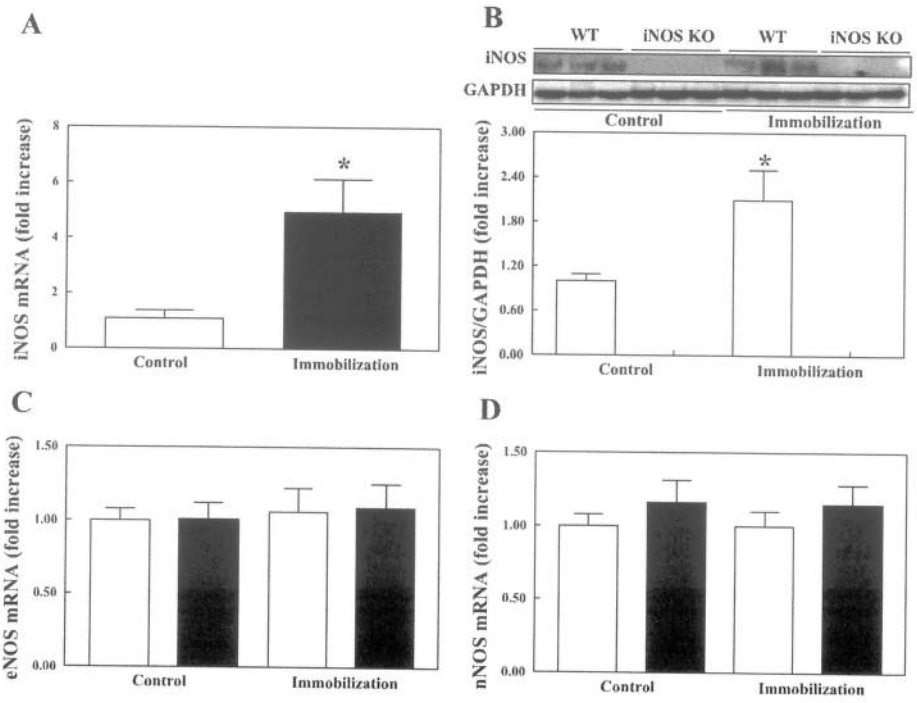

Fig. 2. Gene expression and protein level of nitric oxide synthase (NOS) in skeletal muscle after 1 wk immobilization. Gene expression of inducible NOS (iNOS) was measured in control and immobilized leg in wild-type mice (*A*). Protein level of iNOS was measured in wild-type (open bar) and iNOS knockout (not detected) (*B*). Gene expression of endothelial NOS (eNOS; *C*) and neuronal NOS (nNOS; *D*) was measured in wild-type (open bar) and iNOS knockout mice (filled bar). Data are means ± SE for 11 mice for each group. $^*P < 0.05$ vs. control or wild-type control.

signaling change of protein synthesis preceded that of protein degradation since protein synthesis can be affected earlier than protein degradation (39, 51). The levels of p-Akt and p-mTOR were reduced in both wild-type and iNOS knockout mice by immobilization, and there was no difference between wild-type and iNOS knockout mice after 6 h immobilization (Fig. 3, *A* and *B*). The pAkt and p-mTOR levels after 1 wk immobilization showed the same pattern of changes with that of 6 h immobilization. The p-p70S6K was also reduced by 1 wk immobilization, and there was no difference between wild-type and iNOS knockout mice (Fig. 4, *A–C*). The mRNA expression of MuRF1 and atrogin-1 was not different among the group after 6 h immobilization (Fig. 3, *C* and *D*). Whereas the pFoxO1 level was reduced in wild-type mice after 1 wk immobilization, it was not significantly reduced in iNOS knockout mice (Fig. 5*C*). The mRNA expression and protein levels of MuRF1 and atrogin-1 increased in wild-type mice by 1 wk immobilization. However, lack of iNOS attenuated the

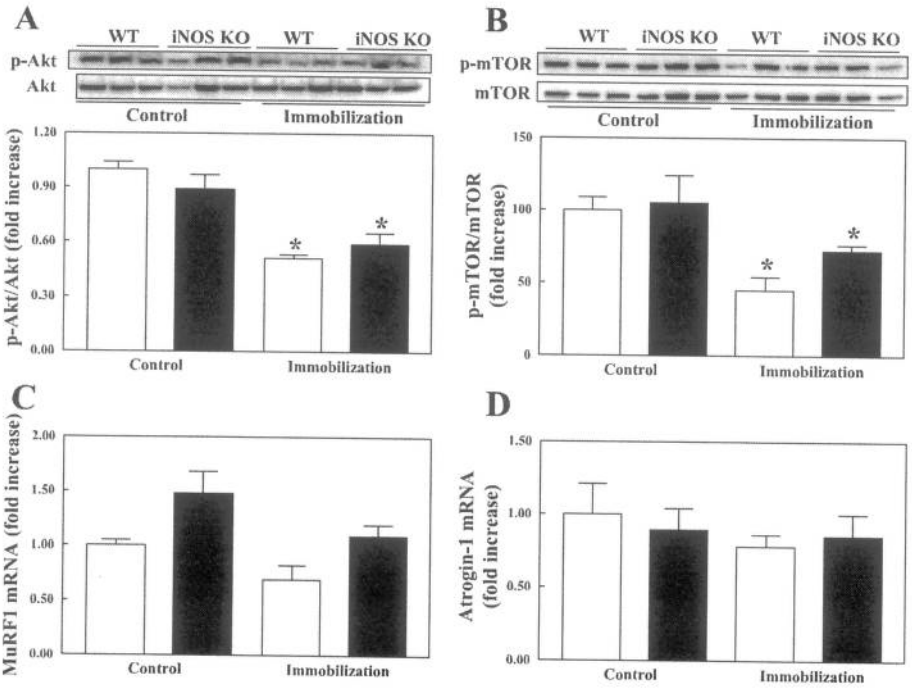

Fig. 3. Phosphorylation of Akt (*A*) and mTOR (*B*) and gene expression of MuRF1 (*C*) and atrogin-1 (*D*) in the skeletal muscle of wild-type (open bar) and inducible nitric oxide synthase knockout (iNOS KO; filled bar) mice after 6 h immobilization. Data are means ± SE for 11 mice for each group. $^*P < 0.05$ vs. wild-type control.

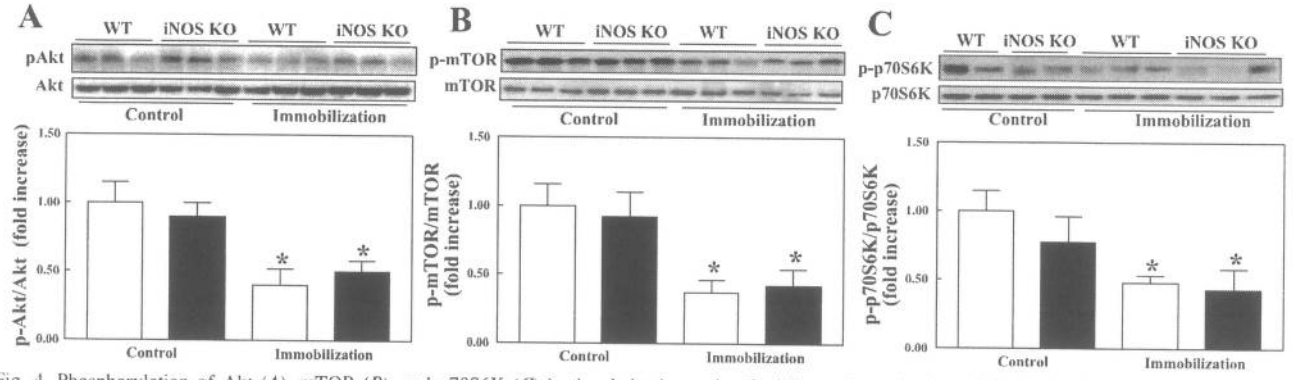

Fig. 4. Phosphorylation of Akt (*A*), mTOR (*B*), and p70S6K (*C*) in the skeletal muscle of wild-type (open bar) and iNOS KO (filled bar) mice after 1 wk immobilization. Data are means ± SE for 7–11 mice for each group. $^*P < 0.05$ vs. wild-type control.

increase of mRNA and protein levels of MuRF1 and atrogin-1 by immobilization (Fig. 5, *D* and *E*).

Oxidative stress. Aconitase activity was measured as a functional indicator of superoxide radicals since aconitase is reversibly oxidized by superoxide, leading to aconitase inactivation (15, 50). While aconitase activity was reduced by 1 wk immobilization in wild-type mice, it was not significantly affected by immobilization in iNOS knockout mice. MnSOD activity was also reduced following 1 wk immobilization, and deficiency of iNOS reversed the decreased MnSOD activity by immobilization. Immobilization significantly increased carbonylated protein level in wild-type mice by immobilization, which was normalized in iNOS knockout mice. Plasma level of the NO metabolites nitrite and nitrate was reduced in iNOS knockout mice. Nitrotyrosine level of the 1-wk immobilized leg was increased compared with that of the control leg in wild-type mice, while it was not increased in iNOS knockout mice. Nitrotyrosine level was lower in iNOS knockout mice in the control group (Fig. 6). These results suggest that immobilization induces oxidative stress, and deficiency of iNOS suppressed immobilization-induced oxidative stress. The activities of ERK and p38 were measured since they are involved in oxidative stress (26). Phosphorylated ERK was increased in wild-type mice by immobilization, while it was not signifi-

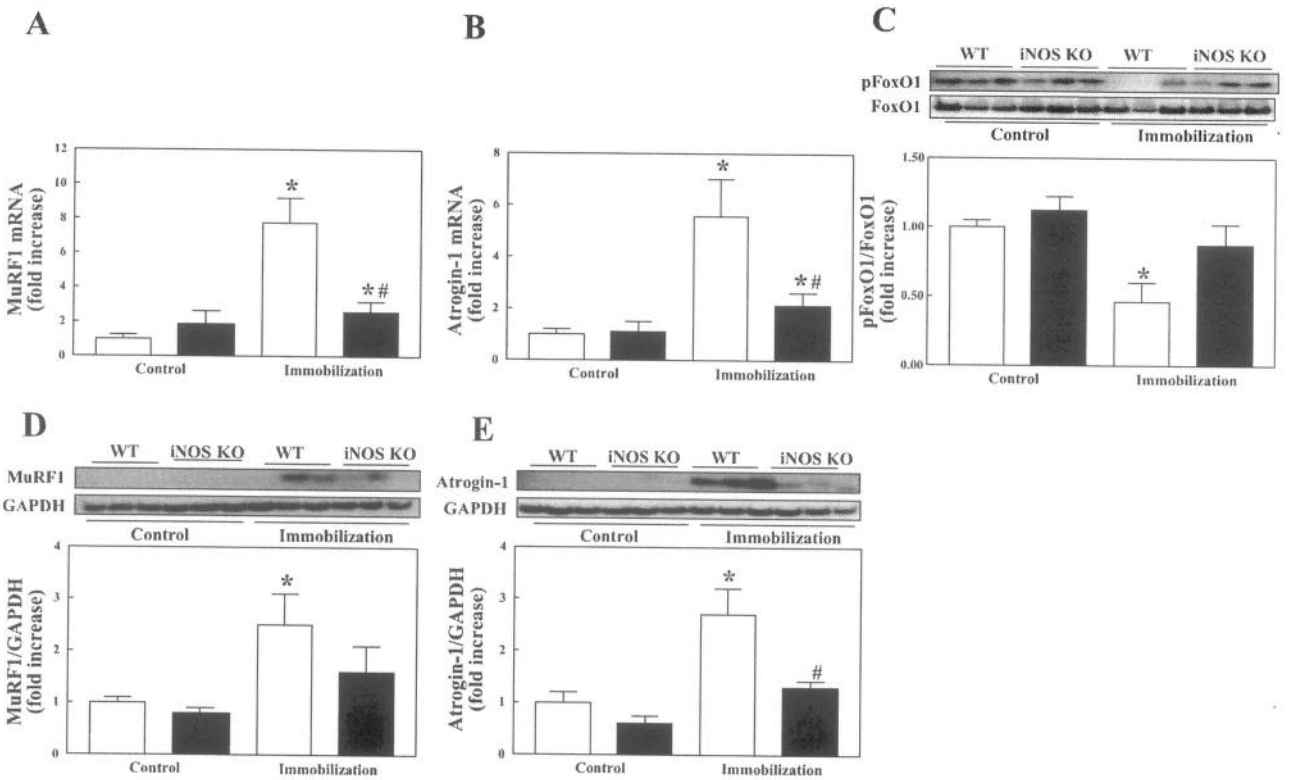

Fig. 5. Gene expression and protein level of MuRF1 (*A*, *D*) and atrogin-1 (*B*, *E*) and phosphorylation of forkhead box O1 (FoxO1; C) in the skeletal muscle of wild-type (open bar) and iNOS KO (filled bar) mice after 1 wk immobilization. Data are means ± SE for 11 mice for each group. $^*P < 0.05$ vs. wild-type control; $\#P < 0.05$ vs. wild-type immobilization.

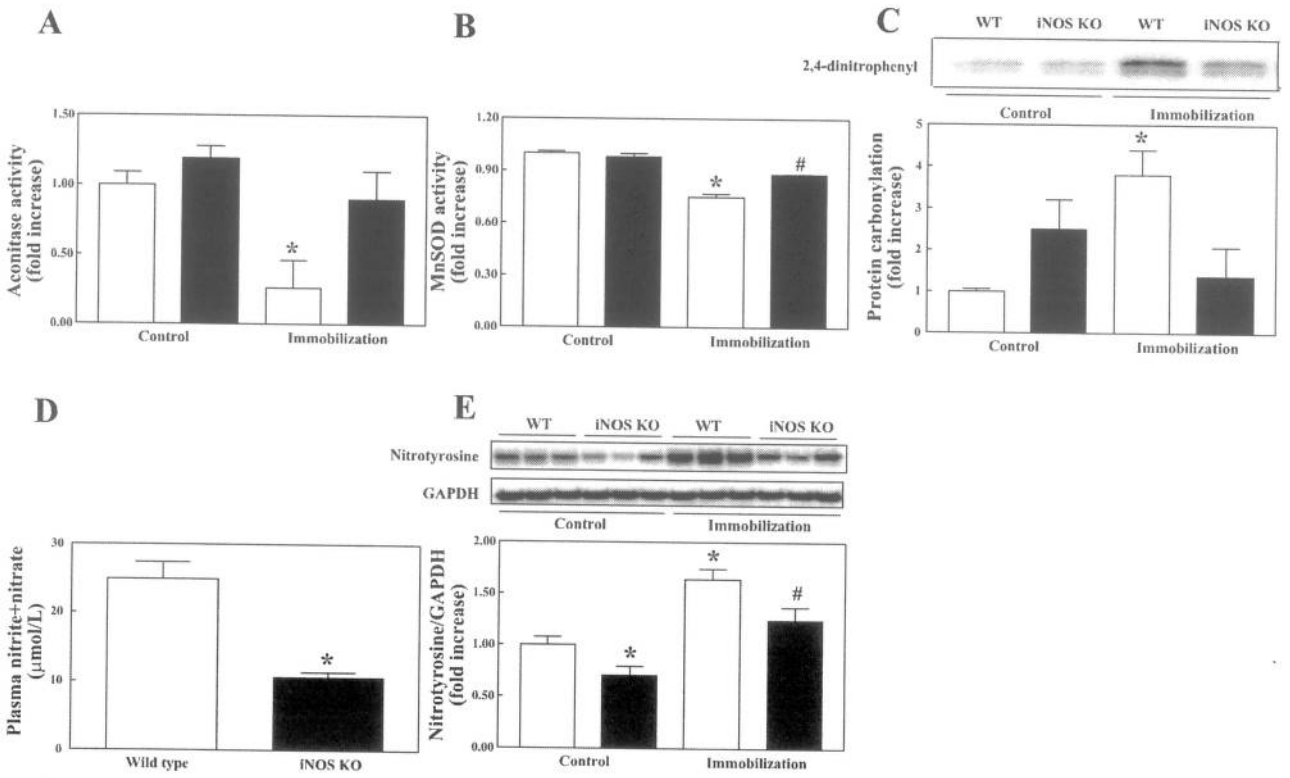

Fig. 6. The level of oxidative stress in skeletal muscle and plasma concentration of nitric oxide metabolites in wild-type (open bar) and iNOS KO (filled bar) mice after 1 wk immobilization. Aconitase activity (*A*), Mn-superoxide dismutase activity (SOD; *B*), protein carbonylation (*C*), nitric oxide metabolites nitrite and nitrate level in plasma (*D*), and nitrotyrosine level (*E*). Data are means ± SE for 7–11 mice for each group. $*P < 0.05$ vs. wild-type or wild-type control. $\#P < 0.05$ vs. wild-type immobilization.

cantly changed in iNOS knockout mice. Phosphorylated p38 (p-p38) showed the same pattern of changes with pERK after 6 h immobilization. The level of pERK in skeletal muscle after 1 wk immobilization showed a similar pattern of changes with that observed at 6 h (Fig. 7).

iNOS inhibition on muscle atrophy. The effect of iNOS deficiency on skeletal muscle atrophy was confirmed by using the selective iNOS inhibitor L-NIL. A 1-wk treatment with L-NIL reduced nitric oxide metabolites in plasma and attenuated the immobilization-induced muscle weight loss in the gastrocnemius and quadriceps muscles. Phosphorylated FoxO1 level was reduced in saline-injected control mice following 1 wk immobilization, and L-NIL treatment attenuated the reduction of pFoxO1 level by immobilization. MuRF1 and atrogin-1 protein levels increased significantly in control mice by immobilization, which were also attenuated by L-NIL treatment (Fig. 8).

DISCUSSION

The present study demonstrates that deficiency of iNOS attenuates immobilization-induced skeletal muscle atrophy that is accompanied by improved contraction-stimulated glucose uptake, suppressed oxidative stress, and reduced MuRF1 and atrogin-1 levels in skeletal muscle. To our knowledge, this is the first study directly showing the causative role of iNOS in muscle atrophy in vivo.

Skeletal muscle mass is maintained by a balance between protein synthesis and protein degradation. Since myofibrillar proteins comprise about 85% of the fiber volume, decreased protein synthesis or/and increased protein degradation leads to muscle atrophy (7, 37). Protein synthesis is regulated by several signaling pathways. The Akt/mTOR/p70S6K pathway plays a crucial role in skeletal muscle protein synthesis (19, 44). Dynamic shortening or lengthening exercise increases protein synthesis that accompanies increased Akt and p70S6K activities in skeletal muscle of healthy man (11). High-intensity leg resistance exercise for 2 h in both men and women increases protein synthesis and activities of Akt, mTOR, and p70S6K in skeletal muscle (12). Furthermore, overexpression of Akt activates mTOR and p70S6K and induces hypertrophy (6), whereas deficiency of Akt induces muscle atrophy in mice (59). Presently, immobilization for 1 wk reduced activities of Akt, mTOR, and p70S6K in hindlimb. Consistent with our result, hindlimb immobilization for 10 days induces skeletal muscle atrophy and decreases the Akt and p70S6K activities (60). These results suggest that reduced protein synthesis is involved in immobilization-induced skeletal muscle atrophy in this study.

Protein degradation is modulated by at least four major proteolytic pathways: lysosomal, Ca^{2+}-dependent, caspase-dependent, and ubiquitin-proteasome-dependent pathways (9). Although all these pathways are involved in skeletal muscle atrophy, accumulating evidence supports the idea that the bulk of myofibrillar protein degradation is mediated by ubiquitin proteasome-dependent pathways during immobilization-induced muscle atrophy (21, 52). Proteins targeted for degrada-

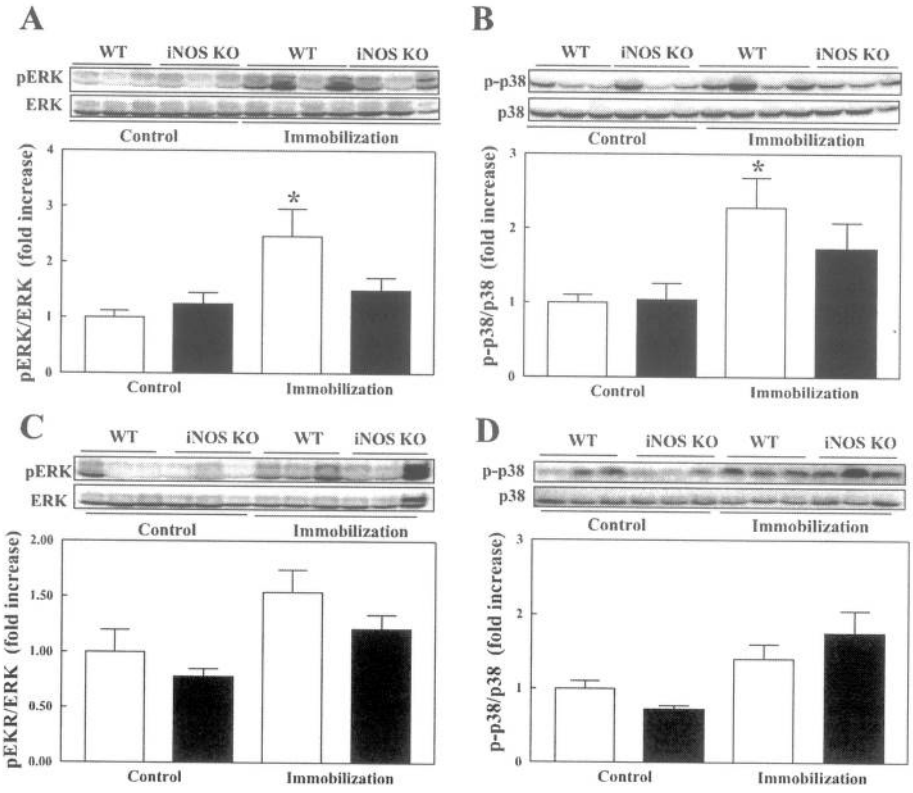

Fig. 7. Phosphorylation of ERK (*A* and *C*) and p38 (*B* and *D*) in the skeletal muscle of wild-type (open bar) and iNOS KO (filled bar) mice. Left hindlimb was immobilized for 6 h (*A* and *B*) or 1 wk (*C* and *D*). Data are means ± SE for 11 mice for each group. *$P < 0.05$ vs. wild-type control.

tion are tagged with ubiquitin and then recognized by proteasomes that degrade the protein by proteolysis (52). For the ubiquitination of protein, the coordinated reaction of three sets of enzymes, ubiquitin-activating enzyme (E1), ubiqutin-conjugating enzyme (E2), and ubiqutin ligases (E3), are required, and the key enzymes in this process are E3 ubiquitin ligases, which functions as the protein recognition component (16, 52). Gene expression of two E3 ubiquitin ligases atrogin-1 and MuRF1 is increased in atrophic skeletal muscles (18). Furthermore, overexpression of atrogin-1 produces atrophy, whereas mice deficient in either atrogin-1 or MuRF1 are found to be resistant to atrophy (5). Regulation of MuRF1 and atrogin-1 is directly or indirectly mediated by FoxOs (44, 45). Although FoxOs are involved in differentiation and metabolism of skeletal muscle, the activities of FoxO1 and FoxO3 are upregulated in various models of atrophy (44). Moreover, overexpression of FoxO1 and FoxO3 increases the expression of MuRF1 and atrogin-1 and reduces muscle mass (24, 43), while knockdown of FoxO1 expression inhibits dexamethasone-induced elevation of atrogin-1 and MuRF1 levels and protein degradation in myotubes (47). In agreement with these previous results, we also presently demonstrated that immobilization for 1 wk increased the FoxO1 activity and MuRF1 and atrogin-1 levels. Since increased expression of these ligases is associated with increased protein degradation, these results suggest that increased protein degradation as well as reduced protein synthesis is involved in skeletal muscle atrophy induced by immobilization. Interestingly, while activities of Akt and mTOR were reduced both after 6 h or 1 wk immobilization, the expression level of these ligases was reduced only after 1 wk immobilization, suggesting that protein synthesis is affected earlier than protein degradation. A previous study consistently showed that muscle atrophy results from a rapid decrease in protein synthesis rate followed by a slower increase in protein degradation (51).

Presently, deficiency of iNOS attenuated immobilization-induced skeletal muscle atrophy that was accompanied with functional recovery assessed by contraction-stimulated glucose uptake. Contraction-stimulated glucose uptake has been reported to correlate with the amount of tension developed by the muscle (22). Accordingly, lower contraction-stimulated glucose uptake in immobilized leg implies reduced tension development and functional deficit of atrophic muscle that was attenuated by deficiency of iNOS. In agreement with our study, the protein level and activity of iNOS in atrophic skeletal muscle of old sedentary rats are increased and exercise normalizes these increments (48). Skeletal muscle of patients with chronic obstructive pulmonary disease and low body weight displays increased nuclear factor-κB activation and iNOS expression (3). Moreover, iNOS has been suggested as a mediator in age-related muscle loss and cytokine-induced cachexia (20). Interestingly, lack of iNOS presently blocked increased gene expression of E3 ubiquitin ligases induced by immobilization, while lack of iNOS had no effect on the decrease of signaling molecules involved in protein synthesis. Accordingly, we propose that iNOS deficiency attenuates immobilization-induced muscle atrophy via reduction of protein degradation.

However, the role of iNOS in skeletal muscle has not been consistently defined previously. Increased iNOS mRNA expression by lipopolysacchride (LPS) is accompanied with suppressed oxidative stress and decreased MuRF1 and atrogin-1 mRNA levels in oxidative soleus muscle, whereas blunted

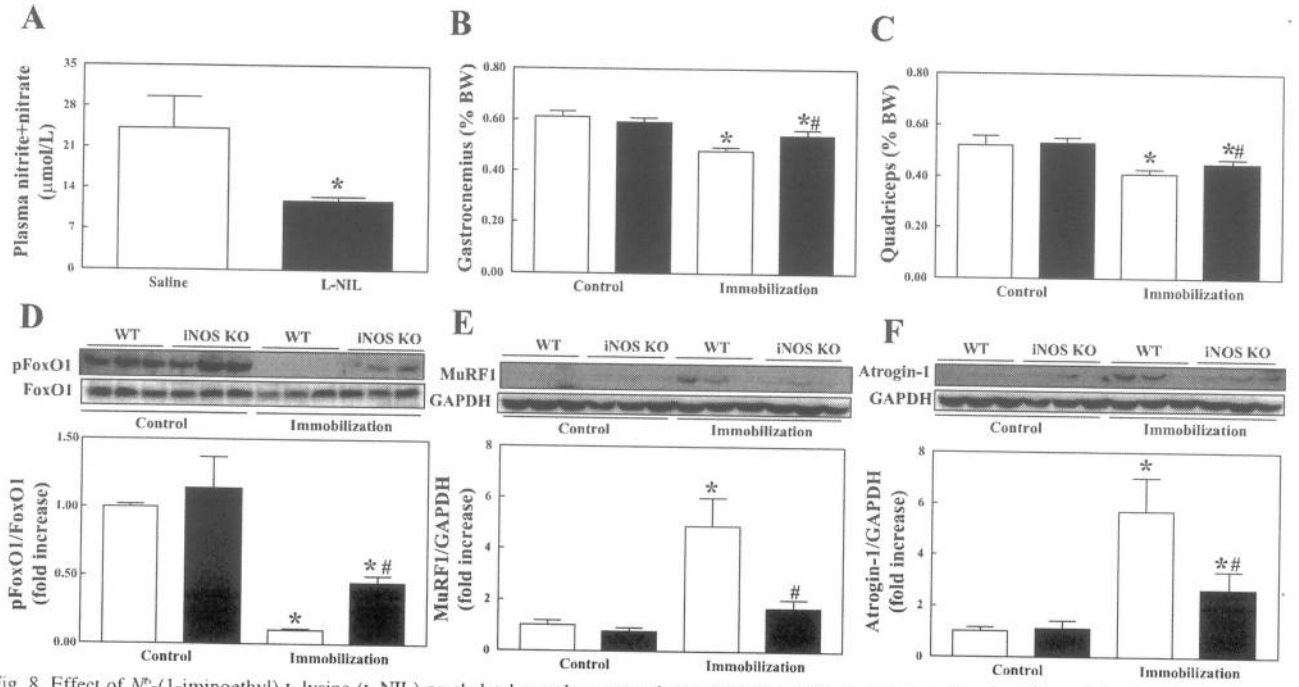

Fig. 8. Effect of N^{ω}-(1-iminoethyl)-L-lysine (L-NIL) on skeletal muscle mass and proteins involved in degradation after 1 wk immobilization. Plasma level of nitric oxide metabolites in saline (open bar)- and L-NIL-injected (filled bar) wild-type mice (*A*). The weights of gastrocnemius (*B*) and quadriceps (*C*) muscles were corrected for body weight (BW). Phosphorylation of forkhead box O1 (FoxO1; *D*) and protein levels of MuRF1 (*E*) and atrogin-1 (*F*) in the skeletal muscle. Data are means ± SE for 11 mice for each group. $*P < 0.05$ vs. saline or saline control; $\#P < 0.05$ vs. saline immobilization.

iNOS response by LPS induces oxidative stress and increased MuRF1 and atrogin-1 mRNA levels in glycolytic white vastus lateralis muscle (61). This protective role of iNOS in soleus muscle atrophy has not been consistently demonstrated previously, and hindlimb unloading for 28 days decreases muscle mass by 55%, which is followed by increased iNOS expression in soleus (29). Presently gastrocnemius and quadriceps muscles, which mostly contain glycolytic fibers, showed increased iNOS expression by immobilization and iNOS deficiency attenuated muscle atrophy. Although the discrepancy in the role of iNOS in muscle atrophy is unclear, the difference of atrophy-inducing factor could partly play a role. The effect of LPS-induced muscle atrophy in iNOS knockout mice remains to elucidate it in a further study.

The underlying mechanisms that are involved in the attenuating effect of lack of iNOS on immobilization are unclear, but reduced oxidative stress may be responsible. Although historically it was believed that the inactive muscle produces less reactive oxygen species (ROS) than actively contracting muscle, accumulating evidence indicates that unused skeletal muscle generates more ROS and oxidative stress functions as one of the causes of skeletal muscle atrophy (40, 46). Hindlimb unloading increases lipid peroxide level and reduces antioxidant enzyme activity such as MnSOD, catalase, and glutathione peroxidase in skeletal muscle (30). Treatment of muscle cells with hydrogen peroxide increases protein degradation (17), and antioxidant treatment attenuates mechanical ventilation-induced muscle atrophy (34). Reduced aconitase and MnSOD activities noted in the present study support increased ROS generation by immobilization. Moreover, increased carbonylated protein in immobilized leg observed in this study also supports the idea that immobilization induces oxidative stress since protein carbonylation in skeletal muscle is increased by oxidative stress, which is associated with protein dysfunction (4). Endogenous production of NO can produce several reactive nitrogen species, including peroxynitrite, which are highly active compounds that cause tissue damage though oxidation and nitration of biomolecules (55). Nitrated tyrosine represents a biological marker for peroxinitrite-induced tissue damage and is increased in aged subjects and inflamed tissues (8, 41). Presently, immobilization increased the nitrotyrosine level, suggesting that immobilization induces nitrosative stress. However, these observed findings, suppressed aconitase and MnSOD activities and increased carbonylated protein and nitrotyrosine levels by immobilization, were reversed in iNOS knockout mice, indicating that immobilization-induced oxidative stress was mitigated by deficiency of iNOS. These results also suggest that iNOS plays an important role in oxidative stress induced by immobilization. Our notion is also supported by our data that immobilization increased activities of p38 and lack of iNOS inhibited the increase of p38 activities that are known to mediate TNF-α-induced atrogin 1 activation in skeletal muscle (32). Moreover, the ERK and p38 signaling pathways are involved in NF-kB transactivation during oxidative stress in skeletal muscle myoblasts (26). The collective data support the suggestion that immobilization increases iNOS expression, which leads to oxidative stress-induced protein degradation.

Overall, deficiency of iNOS attenuates immobilization-induced skeletal muscle atrophy via reduced oxidative stress. Possibly a decrease of protein degradation rather than an increase of protein synthesis is involved in this reaction. These results suggest the possibility of inhibition of iNOS as a target molecule for immobilization-induced muscle atrophy. How-

ever, the role of iNOS in infection and inflammation is diverse, depending on the diseases (38), which should also be considered during the development of iNOS inhibitors as therapeutic agents for muscle atrophy.

ACKNOWLEDGMENTS

We thank Professors Joon Ha Lee and Kyeung Soo Lee for expert advice.

GRANTS

This work was supported by a Korea Science and Engineering Foundation (KOSEF) grant funded by the Korean government (2010-0007389).

DISCLOSURES

No conflicts of interest, financial or otherwise, are declared by the author(s).

AUTHOR CONTRIBUTIONS

Author contributions: S.-K.B., S.-d.K., and S.-Y.P. conception and design of research; S.-K.B., H.-N.C., T.-J.J., and H.S.K. performed experiments; S.-K.B., H.-N.C., T.-J.J., H.S.K., and S.-Y.P. analyzed data; S.-K.B., H.-N.C., T.-J.J., Y.-W.K., Y.-D.K., J.-M.D., J.-Y.K., S.-d.K., and S.-Y.P. interpreted results of experiments; S.-K.B., H.-N.C., T.-J.J., and S.-Y.P. prepared figures; S.-K.B. and S.-Y.P. drafted manuscript; Y.-W.K., J.-M.D., S.-d.K., and S.-Y.P. edited and revised manuscript; Y.-W.K. and S.-Y.P. approved final version of manuscript.

REFERENCES

1. **Abadi A, Glover EI, Isfort RJ, Raha S, Safdar A, Yasuda N, Kaczor JJ, Melov S, Hubbard A, Qu X, Phillips SM, Tarnopolsky M.** Limb immobilization induces a coordinate down-regulation of mitochondrial and other metabolic pathways in men and women. *PLos One* 4: e6518, 2009.
2. **Adams V, Yu J, Mobius-Winkler S, Linke A, Weigl C, Hilbrich L, Schuler G, Hambrecht R.** Increased inducible nitric oxide synthase in skeletal muscle biopsies from patients with chronic heart failure. *Biochem Mol Med* 61: 152–160, 1997.
3. **Agusti A, Morla M, Sauleda J, Saus C, Busquets X.** NF-kappaB activation and iNOS upregulation in skeletal muscle of patients with COPD and low body weight. *Thorax* 59: 483–487, 2004.
4. **Barreiro E, Hussain SN.** Protein carbonylation in skeletal muscles: impact on function. *Antioxid Redox Signal* 12: 417–429, 2010.
5. **Bodine SC, Latres E, Baumhueter S, Lai VK, Nunez L, Clarke BA, Poueymirou WT, Panaro FJ, Na E, Dharmarajan K, Pan ZQ, Valenzuela DM, DeChiara TM, Stitt TN, Yancopoulos GD, Glass DJ.** Identification of ubiquitin ligases required for skeletal muscle atrophy. *Science* 294: 1704–1708, 2001.
6. **Bodine SC, Stitt TN, Gonzalez M, Kline WO, Stover GL, Bauerlein R, Zlotchenko E, Scrimgeour A, Lawrence JC, Glass DJ, Yancopoulos GD.** Akt/mTOR pathway is a crucial regulator of skeletal muscle hypertrophy and can prevent muscle atrophy in vivo. *Nat Cell Biol* 3: 1014–1019, 2001.
7. **Boonyarom O, Inui K.** Atrophy and hypertrophy of skeletal muscles: structural and functional aspects. *Acta Physiol (Oxf)* 188: 77–89, 2006.
8. **Cha HN, Kim YW, Kim JY, Kim YD, Song IH, Min KN, Park SY.** Lack of inducible nitric oxide synthase does not prevent aging-associated insulin resistance. *Exp Gerontol* 45: 711–718, 2010.
9. **Combaret L, Dardevet D, Bechet D, Taillandier D, Mosoni L, Attaix D.** Skeletal muscle proteolysis in aging. *Curr Opin Clin Nutr Metab Care* 12: 37–41, 2009.
10. **Connor JR, Manning PT, Settle SL, Moore WM, Jerome GM, Webber RK, Tjoeng FS, Currie MG.** Suppression of adjuvant-induced arthritis by selective inhibition of inducible nitric oxide synthase. *Eur J Pharmacol* 273: 15–24, 1995.
11. **Cuthbertson DJ, Babraj J, Smith K, Wilkes E, Fedele MJ, Esser K, Rennie M.** Anabolic signaling and protein synthesis in human skeletal muscle after dynamic shortening or lengthening exercise. *Am J Physiol Endocrinol Metab* 290: E731–E738, 2006.
12. **Dreyer HC, Fujita S, Glynn EL, Drummond MJ, Volpi E, Rasmussen BB.** Resistance exercise increases leg muscle protein synthesis and mTOR signalling independent of sex. *Acta Physiol (Oxf)* 199: 71–81, 2010.
13. **Frimel TN, Kapadia F, Gaidosh GS, Li Y, Walter GA, Vandenborne K.** A model of muscle atrophy using cast immobilization in mice. *Muscle Nerve* 32: 672–674, 2005.
14. **Fujimoto M, Shimizu N, Kunii K, Martyn JA, Ueki K, Kaneki M.** A role for iNOS in fasting hyperglycemia and impaired insulin signaling in the liver of obese diabetic mice. *Diabetes* 54: 1340–1348, 2005.
15. **Gardner PR, Fridovich I.** Inactivation-reactivation of aconitase in *Escherichia coli*. A sensitive measure of superoxide radical. *J Biol Chem* 267: 8757–8763, 1992.
16. **Glass DJ.** Signaling pathways perturbing muscle mass. *Curr Opin Clin Nutr Metab Care* 13: 225–229, 2010.
17. **Gomes-Marcondes MC, Tisdale MJ.** Induction of protein catabolism and the ubiquitin-proteasome pathway by mild oxidative stress. *Cancer Lett* 180: 69–74, 2002.
18. **Gomes MD, Lecker SH, Jagoe RT, Navon A, Goldberg AL.** Atrogin-1, a muscle-specific F-box protein highly expressed during muscle atrophy. *Proc Natl Acad Sci USA* 98: 14440–14445, 2001.
19. **Goodman CA, Mayhew DL, Hornberger TA.** Recent progress toward understanding the molecular mechanisms that regulate skeletal muscle mass. *Cell Signal* 23: 1896–1906, 2011.
20. **Hall DT, Ma JF, Marco SD, Gallouzi IE.** Inducible nitric oxide synthase (iNOS) in muscle wasting syndrome, sarcopenia, and cachexia. *Aging (Albany NY)* 3: 702–715, 2011.
21. **Hasselgren PO, Wray C, Mammen J.** Molecular regulation of muscle cachexia: it may be more than the proteasome. *Biochem Biophys Res Commun* 290: 1–10, 2002.
22. **Ihlemann J, Ploug T, Hellsten Y, Galbo H.** Effect of tension on contraction-induced glucose transport in rat skeletal muscle. *Am J Physiol Endocrinol Metab* 277: E208–E214, 1999.
23. **Jackman RW, Kandarian SC.** The molecular basis of skeletal muscle atrophy. *Am J Physiol Cell Physiol* 287: C834–C843, 2004.
24. **Kamei Y, Miura S, Suzuki M, Kai Y, Mizukami J, Taniguchi T, Mochida K, Hata T, Matsuda J, Aburatani H, Nishino I, Ezaki O.** Skeletal muscle FOXO1 (FKHR) transgenic mice have less skeletal muscle mass, down-regulated Type I (slow twitch/red muscle) fiber genes, and impaired glycemic control. *J Biol Chem* 279: 41114–41123, 2004.
25. **Kandarian SC, Jackman RW.** Intracellular signaling during skeletal muscle atrophy. *Muscle Nerve* 33: 155–165, 2006.
26. **Kefaloyianni E, Gaitanaki C, Beis I.** ERK1/2 and p38-MAPK signalling pathways, through MSK1, are involved in NF-kappaB transactivation during oxidative stress in skeletal myoblasts. *Cell Signal* 18: 2238–2251, 2006.
27. **Kelly RA, Balligand JL, Smith TW.** Nitric oxide and cardiac function. *Circ Res* 79: 363–380, 1996.
28. **Kramer HF, Witczak CA, Taylor EB, Fujii N, Hirshman MF, Goodyear LJ.** AS160 regulates insulin- and contraction-stimulated glucose uptake in mouse skeletal muscle. *J Biol Chem* 281: 31478–31485, 2006.
29. **Lawler JM, Kwak HB, Kim JH, Lee Y, Hord JM, Martinez DA.** Biphasic stress response in the soleus during reloading following hindlimb unloading. *Med Sci Sports Exerc* 44: 600–609, 2012.
30. **Lawler JM, Song W, Demaree SR.** Hindlimb unloading increases oxidative stress and disrupts antioxidant capacity in skeletal muscle. *Free Radic Biol Med* 35: 9–16, 2003.
31. **Li H, Malhotra S, Kumar A.** Nuclear factor-kappa B signaling in skeletal muscle atrophy. *J Mol Med* 86: 1113–1126, 2008.
32. **Li YP, Chen Y, John J, Moylan J, Jin B, Mann DL, Reid MB.** TNF-alpha acts via p38 MAPK to stimulate expression of the ubiquitin ligase atrogin1/MAFbx in skeletal muscle. *FASEB J* 19: 362–370, 2005.
33. **Madaro L, Smeriglio P, Molinaro M, Bouche M.** Unilateral immobilization: a simple model of limb atrophy in mice. *Basic Appl Myol* 18: 149–153, 2008.
34. **McClung JM, Whidden MA, Kavazis AN, Falk DJ, Deruisseau KC, Powers SK.** Redox regulation of diaphragm proteolysis during mechanical ventilation. *Am J Physiol Regul Integr Comp Physiol* 294: R1608–R1617, 2008.
35. **McConell GK, Wadley GD.** Potential role of nitric oxide in contraction-stimulated glucose uptake and mitochondrial biogenesis in skeletal muscle. *Clin Exp Pharmacol Physiol* 35: 1488–1492, 2008.
36. **Moncada S, Higgs A.** The L-arginine-nitric oxide pathway. *N Engl J Med* 329: 2002–2012, 1993.
37. **Morris CA, Morris LD, Kennedy AR, Sweeney HL.** Attenuation of skeletal muscle atrophy via protease inhibition. *J Appl Physiol* 99: 1719–1727, 2005.

38. **Nathan C.** Inducible nitric oxide synthase: what difference does it make? *J Clin Invest* 100: 2417–2423, 1997.
39. **Parkington JD, Siebert AP, LeBrasseur NK, Fielding RA.** Differential activation of mTOR signaling by contractile activity in skeletal muscle. *Am J Physiol Regul Integr Comp Physiol* 285: R1086–R1090, 2003.
40. **Powers SK, Kavazis AN, DeRuisseau KC.** Mechanisms of disuse muscle atrophy: role of oxidative stress. *Am J Physiol Regul Integr Comp Physiol* 288: R337–R344, 2005.
41. **Rabuel C, Samuel JL, Lortat-Jacob B, Marotte F, Lanone S, Keyser C, Lessana A, Payen D, Mebazaa A.** Activation of the ubiquitin proteolytic pathway in human septic heart and diaphragm. *Cardiovasc Pathol* 19: 158–164, 2010.
42. **Reid MB.** Role of nitric oxide in skeletal muscle: synthesis, distribution and functional importance. *Acta Physiol Scand* 162: 401–409, 1998.
43. **Romanello V, Guadagnin E, Gomes L, Roder I, Sandri C, Petersen Y, Milan G, Masiero E, Del Piccolo P, Foretz M, Scorrano L, Rudolf R, Sandri M.** Mitochondrial fission and remodelling contributes to muscle atrophy. *EMBO J* 29: 1774–1785, 2010.
44. **Sandri M.** Signaling in muscle atrophy and hypertrophy. *Physiology (Bethesda)* 23: 160–170, 2008.
45. **Sandri M, Sandri C, Gilbert A, Skurk C, Calabria E, Picard A, Walsh K, Schiaffino S, Lecker SH, Goldberg AL.** Foxo transcription factors induce the atrophy-related ubiquitin ligase atrogin-1 and cause skeletal muscle atrophy. *Cell* 117: 399–412, 2004.
46. **Siu PM, Pistilli EE, Alway SE.** Age-dependent increase in oxidative stress in gastrocnemius muscle with unloading. *J Appl Physiol* 105: 1695–1705, 2008.
47. **Smith IJ, Alamdari N, O'Neal P, Gonnella P, Aversa Z, Hasselgren PO.** Sepsis increases the expression and activity of the transcription factor Forkhead Box O 1 (FOXO1) in skeletal muscle by a glucocorticoid-dependent mechanism. *Int J Biochem Cell Biol* 42: 701–711, 2010.
48. **Song W, Kwak HB, Kim JH, Lawler JM.** Exercise training modulates the nitric oxide synthase profile in skeletal muscle from old rats. *J Gerontol A Biol Sci Med Sci* 64: 540–549, 2009.
49. **Sung HK, Kim YW, Choi SJ, Kim JY, Jeune KH, Won KC, Kim JK, Koh GY, Park SY.** COMP-angiopoietin-1 enhances skeletal muscle blood flow and insulin sensitivity in mice. *Am J Physiol Endocrinol Metab* 297: E402–E409, 2009.
50. **Tarpey MM, Wink DA, Grisham MB.** Methods for detection of reactive metabolites of oxygen and nitrogen: in vitro and in vivo considerations. *Am J Physiol Regul Integr Comp Physiol* 286: R431–R444, 2004.
51. **Thomason DB, Booth FW.** Atrophy of the soleus muscle by hindlimb unweighting. *J Appl Physiol* 68: 1–12, 1990.
52. **Tisdale MJ.** The ubiquitin-proteasome pathway as a therapeutic target for muscle wasting. *J Support Oncol* 3: 209–217, 2005.
53. **Torres SH, De Sanctis JB, de LBM, Hernandez N, Finol HJ.** Inflammation and nitric oxide production in skeletal muscle of type 2 diabetic patients. *J Endocrinol* 181: 419–427, 2004.
54. **Tsuchiya K, Sakai H, Suzuki N, Iwashima F, Yoshimoto T, Shichiri M, Hirata Y.** Chronic blockade of nitric oxide synthesis reduces adiposity and improves insulin resistance in high fat-induced obese mice. *Endocrinology* 148: 4548–4556, 2007.
55. **Valko M, Leibfritz D, Moncol J, Cronin MT, Mazur M, Telser J.** Free radicals and antioxidants in normal physiological functions and human disease. *Int J Biochem Cell Biol* 39: 44–84, 2007.
56. **Vander Lugt JT, Gomez-Marquez J, Caldon J, Louters LL.** Combined effects of troglitazone and muscle contraction on insulin sensitization in Balb-c mouse muscle. *Biochimie* 83: 445–451, 2001.
57. **Wang J, Chu H, Zhao H, Cheng X, Liu Y, Jin W, Zhao J, Liu B, Ding Y, Ma H.** Nitric oxide synthase-induced oxidative stress in prolonged alcoholic myopathies of rats. *Mol Cell Biochem* 304: 135–142, 2007.
58. **Yang X, Ma N, Szabolcs MJ, Zhong J, Athan E, Sciacca RR, Michler RE, Anderson GD, Wiese JF, Leahy KM, Gregory S, Cannon PJ.** Upregulation of COX-2 during cardiac allograft rejection. *Circulation* 101: 430–438, 2000.
59. **Yang ZZ, Tschopp O, Baudry A, Dummler B, Hynx D, Hemmings BA.** Physiological functions of protein kinase B/Akt. *Biochem Soc Trans* 32: 350–354, 2004.
60. **You JS, Park MN, Song W, Lee YS.** Dietary fish oil alleviates soleus atrophy during immobilization in association with Akt signaling to p70s6k and E3 ubiquitin ligases in rats. *Appl Physiol Nutr Metab* 35: 310–318, 2010.
61. **Yu Z, Li P, Zhang M, Hannink M, Stamler JS, Yan Z.** Fiber type-specific nitric oxide protects oxidative myofibers against cachectic stimuli. *PLos One* 3: e2086, 2008.
62. **Zhang P, Chen X, Fan M.** Signaling mechanisms involved in disuse muscle atrophy. *Med Hypotheses* 69: 310–321, 2007.